

V.B.1 Water Transport Exploratory Studies

Rod Borup¹ (Primary Contact),
Rangachary Mukundan¹, John Davey¹,
Roger Lujan¹, Jacob Spendelow¹,
Joe Fairweather¹, Dusan Spornjak¹,
Tom Springer¹, Muhammad Arif²,
David Jacobson², Daniel Hussey²,
Ken Chen³, Karren More⁴, David Wood⁴,
Partha Mukherjee⁴, Peter Wilde⁵,
Ruediger-Bernd Schweiss⁵, Tom Zawodzinski⁶,
Peter Olapade⁷, Jeremy Meyers⁷, Adam Weber⁸

¹Los Alamos National Laboratory
MS D429, P.O. Box 1663
Los Alamos, NM 87545
Phone: (505) 667-2823
E-mail: Borup@lanl.gov

DOE Technology Development Manager:
Nancy Garland

Phone: (202) 586-5673
E-mail: Nancy.Garland@ee.doe.gov

Subcontractors:

- ² National Institute of Standards and Technology (NIST), Gaithersburg, MD
- ³ Sandia National Laboratories, Albuquerque, NM
- ⁴ Oak Ridge National Laboratory, Oak Ridge TN
- ⁵ SGL Technologies GmbH, 86405 Meitingen/Germany
- ⁶ University of Tennessee, Knoxville TN
- ⁷ University of Texas at Austin, Austin, TX
- ⁸ Lawrence Berkeley National Laboratory, Berkeley, CA

Start Date: March 2007
Project End Date: 2011

Objectives

- Develop understanding of water transport in polymer electrolyte membrane (PEM) fuel cells.
- Evaluate properties of materials affecting water transport and fuel cell performance.
- Develop (enable) new components and operating methods.
- Accurately model water transport within the fuel cell.
- Develop a better understanding of freeze/thaw cycles and sub-freezing operation.

Technical Barriers

This project addresses the following technical barriers from the Fuel Cells section of the Fuel Cell Technologies Program Multi-Year Research, Development and Demonstration Plan:

(D) Water Transport within the Stack

Fuel Cell Stack Technical Targets

- Energy efficiency (65% at 25% rated power, 55% at 100% rated power)
- Power density (2,000 Watt/Liter)
- Specific power (2,000 Watt/kg)
- Cost (\$25/kWe)
- Start-up time to 50% power (30 seconds from -20°C, 5 seconds from 20°C)
- Freeze-start operation (Unassisted start from -40°C)

Accomplishments

Gas Diffusion Layer (GDL) Materials

- Demonstrated better water removal characteristics with modified microporous layer (MPL) properties.
- Demonstrated performance improvement by optimizing GDL properties and in-plane GDL type in relation to its flow-field position.

Membrane Water Content Measurements (by Neutron Imaging)

- Measured compression effect on water content in membranes.
- Made reversible in situ measurements of membrane water content to examine Schroeder's paradox.

Freeze

- Measured durability of various cell configurations and the location of frozen water (ice) for various operating conditions.

Modeling

- Created modeling simulations of oxygen partial pressure in the cathode catalyst layer as a function of channel liquid pressure for various types of GDLs.
- Modeled the dynamic behavior of water in response to various step-changes in current density.



Introduction

Ineffective control of water distribution can be a major impediment to implementation of PEM fuel cells (PEMFCs). Several important parameters, including membrane conductivity and mass transfer resistance within porous electrodes, are intimately linked to water distribution, requiring effective management of water in

order to maximize fuel cell performance. Components such as the PEMs and electrode layers require sufficient water to be present in order to allow adequate proton conductivity. Conversely, excess water within the system leads to mass transfer losses and can require additional balance-of-plant costs (extra energy or weight for increased humidification). The range of conditions under which the system is required to operate makes meeting all these requirements at the same time even more difficult. The conditional extremes provide the biggest challenges: maintaining hydration under hot/dry conditions and preventing flooding/dealing with ice formation under cold/wet conditions. In order to address these challenges there is a need for increased understanding of water transport and phase change within fuel cell components. This requires that the structure and properties of fuel cell materials be fully understood. The materials ultimately employed will need durability under normal and transient operations while allowing effective water management under any environmentally-relevant condition.

Approach

Our approach to understanding water transport within fuel cells is structured in three areas: fuel cell studies, characterization of component water transport properties, and modeling of water transport. These areas have aspects that can be considered free-standing, but each benefit greatly from work performed in the other areas. The modeling studies tie together what is learned during component characterization and allow better interpretation of the fuel cell studies. This approach and our team give us the greatest chance to increase the understanding of water transport in fuel cells and to develop and employ materials that will overcome water-related limitations in fuel cell systems.

Results

Effect of Hydrophilic Treatment of Microporous Layer on Fuel Cell Performance

The GDL in a PEMFC is the component primarily responsible for effective water management under a wide variety of conditions. Optimal GDL performance is obtained when the MPL has enough hydrophobic pores for gas access and enough hydrophilic pores for water wicking [1]. To optimize the water transport properties of the GDL, SGL Technologies has developed new GDLs that incorporate aluminosilicate fibers to create hydrophilic pathways in the MPL to facilitate liquid water removal from the cathode catalyst layer [2]. Figure 1a shows the performance of fuel cells using the GDL with the hydrophilic fibers in the MPL (25BL) is significantly better than the baseline hydrophobic GDL

(25BC). The cell with the 25BL GDL shows a 150 mV improvement in the voltage at a current density of 2 A cm^{-2} . However when the cathode gas was changed to HelOx, the performance of the two cells were almost identical. This indicates that the improvement in the performance is primarily due to better mass transport characteristics of the 25BL GDL with the hydrophilic fibers in the MPL.

The improvement in mass transport was verified with alternating current impedance spectra of the two cells which confirms the better mass transport for the 25BL GDL and is illustrated in Figure 1b. The high frequency resistance (HFR) of both these cells is the same ($\approx 0.04 \text{ } \Omega \text{ cm}^2$), however, the low frequency (0.1 Hz) resistance of the cell with the 25BL GDL is $\approx 40\%$ lower. Moreover, the impedance spectra in HelOx of these two cells is identical, indicating that the improved performance of the 25BL GDL is due to better water removal resulting in improved oxygen diffusion kinetics. The decreased mass transport resistance in HelOx when compared to air is directly attributed to the 3.7 times better diffusion of O_2 in He vs N_2 [3].

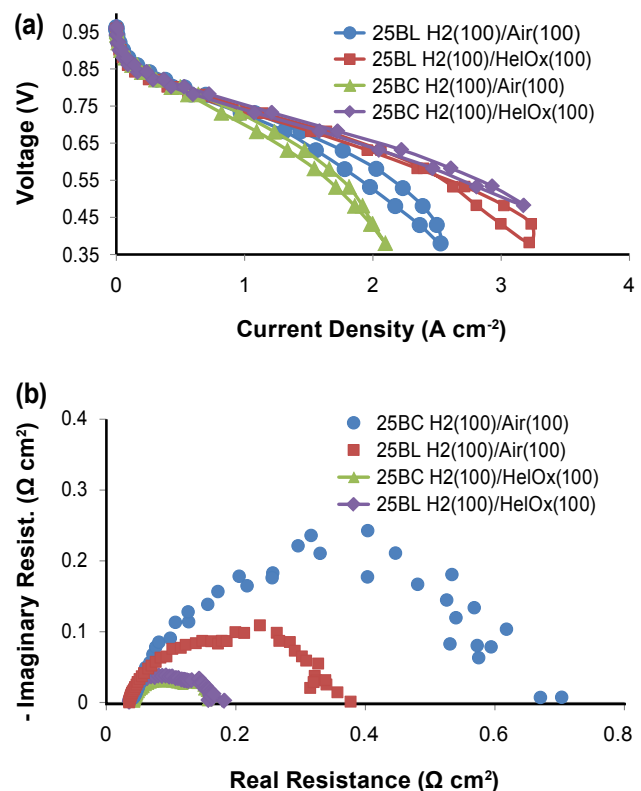


FIGURE 1. (a) Polarization curves for GDLs 25BC and 25BL and (b) Alternating current impedance spectra (0.1 Hz to 1 kHz) obtained at 80°C , at 1.4 A cm^{-2} , 100% inlet relative humidity (RH) with anode stoichiometry 1.2 and cathode stoichiometry 2.0 and 40 psia outlet pressure.

Neutron Imaging of MEA Water Profiles

In order to further investigate the origin of the mass transport improvement, the water profiles of two cells with 24BC and 25BL GDLs were obtained via neutron radiography with the newly installed 13 μm resolution detector at NIST. The 25BC cell is expected to behave similar to the 24BC one (based on the performance data). Figure 2 shows the water profiles obtained in the cross-section view of these cells. The baseline GDL (24BC) shows a typical profile where a peak in water content is seen close to the location of the cathode catalyst layer. Moreover the MPL ($\approx 50 \mu\text{m}$ thick) exhibits low liquid water content as illustrated by the steep drop in water content as one moves away from the membrane electrode assembly (MEA). In contrast, the cell with the 25BL GDL shows significant liquid water in the MPL region as evidenced by the steady water content profile as one moves across the MPL. This figure also indicates that the liquid water saturation in the cathode catalyst layer is lower when using the 25BL GDL. Both GDLs show significant water accumulation in the substrate with the 25BL GDL having greater water saturation. The water content indicates a maximum saturation of only 15% in the GDL substrate for the 25BL GDL. Although the absolute water content in the thin catalyst layers and membranes is difficult to obtain due to the smearing of the water content based on the 13 mm detector resolution, these results indicate that the mass transport losses are predominantly due to liquid water in the catalyst layer pores.

Modeling of GDL Properties Effect

Modeling simulations examined various GDL properties to evaluate the mass-transfer limiting current as a function of inlet water flux. Results show that there are high limiting currents and the water flux is flat in the

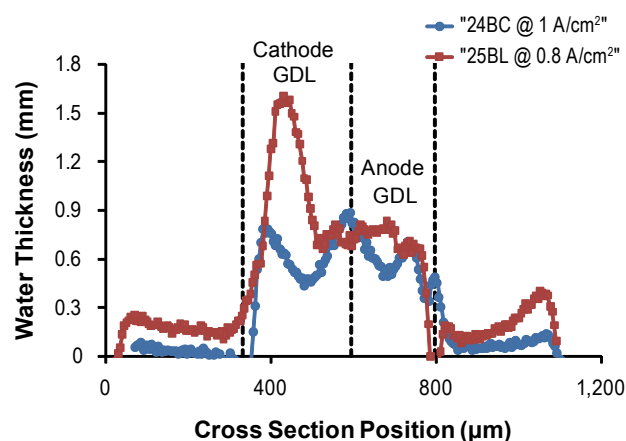


FIGURE 2. Water profiles in 2.5 cm² fuel cells operated at 80°C (100% inlet RH) using the two GDLs. 25BL (hydrophilic fibers in MPL) and 25BC (hydrophobic MPL)

practical fuel cell operating range. The modeling results agree with the experimental results, showing that bulk transport (convection) does not lead to mass-transfer limitations because the effective permeability remains too high. These results indicate that once a water pathway is established, it can sustain practical liquid-water fluxes. The effect of variations in GDL properties on mass transport can be summarized in Figure 3, which shows the oxygen partial pressure as a function of the channel water pressure. At high channel water pressures, the GDL with hydrophilic pores retains the highest oxygen partial pressures at the catalyst layer.

Neutron Imaging of Membrane Water Content

Water transport in the Nafion[®] ionomeric membrane has profound influence on the performance of the polymer electrolyte fuel cell, in terms of internal resistance and overall water balance. We conducted high resolution neutron imaging of Nafion[®] membranes in order to measure water content in situ with varied compression on the membrane. Figure 4 shows the measured membrane water content ($\lambda = \#$ water molecules per sulfonic acid group) for various cell compressions, including a restricted membrane (low membrane compression, <140 psi) and a highly compressed membrane (>400 psi). Restricted and compressed membranes have identical water content with the exception of when the membrane was in contact with liquid H₂O. In contact with liquid water, the highly compressed membrane had substantially less water ($\lambda = 17.5$) than the membrane that had lower compressions ($\lambda = 21.5$), indicated that compression can limit the membrane water uptake, but only at high water contents. When comparing the constrained

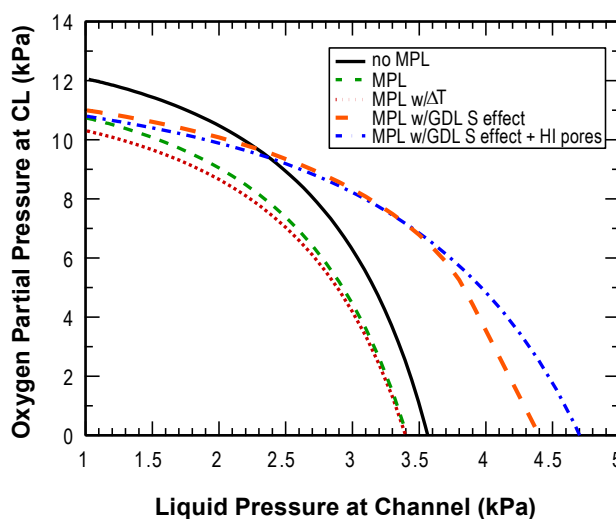


FIGURE 3. Modeling simulations of oxygen partial pressure in the cathode catalyst layer as a function of channel liquid pressure for various types of GDLs.

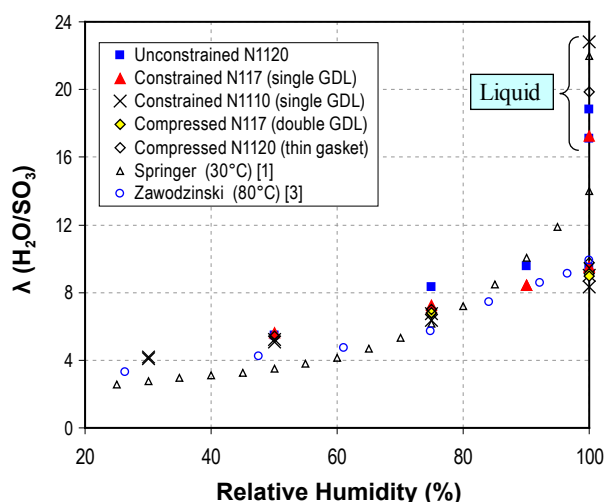


FIGURE 4. In situ neutron imaging measurement of membrane water content for a restricted membrane (low membrane compression, <140 psi) and a compressed membrane (>400 psi).

and compressed cases, it is interesting that additional membrane compression did not cause significant reduction in water uptake. A possible explanation may be that the compression of the GDL mitigates the pressure exerted on the membrane itself. The in situ measurement ability of neutron imaging was also used to examine Schroeder's paradox, which addresses the inconsistency between the measured membrane water content at 100% RH and in contact with liquid water, which is inconsistent with thermodynamics because the chemical potential of saturated water vapor is equal to that of liquid water at the same temperature. For this measurement, the membrane RH was increased from 50% RH to 100% RH to liquid, then reversed. The membrane water content at 100% RH was identical in the forward and reverse directions at $\lambda = 10$, compared with the liquid $\lambda = 21.5$, thus proving the validity of Schroeder's paradox.

Conclusions

GDL Materials

- Modified MPL properties show better water removal characteristics and performance.
- Performance improvement can be realized by varying the in-plane GDL type in relation to its flow-field position.
- Mass transport losses are predominantly due to liquid water in the catalyst layer pores, not due to water saturation levels in the GDL substrate.

Membrane Water Content Measurements by Neutron Imaging

- Cell compression influences membrane water content at high levels of water.
- Reversible in situ measurements of membrane water content verified existence of Schroeder's paradox in Nafion[®] fuel cell MEAs.

Freeze

- Membrane hydration due to the generated current and back diffusion is dominant at sub-freezing temperatures.
- Freeze operation/cycling can result in loss of catalyst surface area, increase in porosity of catalyst layer and mass transfer limitations.
- High Teflon[®] content in the MPL results in better durability during freeze/thaw cycling and operation.
- Ice formation location depends on temperature, current density, cell configuration.

Future Directions

Experimental and Characterization

- Segmented cell measurements of new optimized GDL materials (25BL).
- Pneumatic pressure control to change in situ GDL compression and measure GDL compression effect on water transport.
- X-ray radiography/tomography of GDLs measuring water movement through pores.

Modeling

- Modeling of through-plane water distribution and transport in MEA-GDL regions by simulating water profile measurements with varying conditions and GDL hydrophobicity.

Transport Projects

- Support new transport projects and distribute measurements to 2008-funded projects.

FY 2010 Publications/Presentations

1. J. Mishler, Y. Wang, R. Mukundan, R. Borup, D.S. Hussey, D.L. Jacobson, In situ Investigation of Water Distribution in Polymer Electrolyte Fuel Cell Using Neutron Radiography, submitted to 2010 ECS Transactions.
2. R. Mukundan, J.R. Davey, J.D. Fairweather, D. Spornjak, J. Spendelow, D.S. Hussey, D.L. Jacobson, P. Wilde, R. Schweiss, and R.L. Borup, Effect of Hydrophilic Treatment of Microporous Layer on Fuel Cell Performance, submitted to 2010 ECS Transactions.

3. P.O. Olapade, R. Mukundan, J.R. Davey, R.L. Borup and J.P. Meyers, Modeling the Dynamic Behavior of Proton-Exchange Membrane Fuel Cell, submitted to 2010 ECS Transactions.
4. P.P. Mukherjee, E. Shim, R. Mukundan, and R.L. Borup, Digital Volume Imaging of the PEFC Gas Diffusion Layer, submitted to 2010 ECS Transactions.
5. Y. Wang, P.P. Mukherjee, J. Mishler, R. Mukundan, R.L. Borup, Cold start of polymer electrolyte fuel cells: Three-stage startup characterization. *Electrochimica Acta* (2010), 55(8), 2636-2644.
6. D.L. Wood, C. Rulison, R.L. Borup, Surface Properties of PEMFC Gas Diffusion Layers. *Journal of the Electrochemical Society* (2010), 157(2), B195-B206.
7. D.L. Wood, J. Chlistunoff, J. Majewski, R.L. Borup, Nafion Structural Phenomena at Platinum and Carbon Interfaces. *Journal of the American Chemical Society* (2009), 131(50), 18096-18104.
8. D.L. Wood, R. Mukundan, R.L. Borup, In-plane mass-transport studies of GDL variation using the segmented cell approach. *ECS Transactions* (2009), 25(1, Proton Exchange Membrane Fuel Cells 9), 1495-1506.
9. J.R. Davey, R. Mukundan, J.S. Spendelow, P.P. Mukherjee, D.S. Hussey, D.L. Jacobson, M. Arif, R.L. Borup, Wetting and drying responses of gas diffusion layers and proton exchange membrane to current transients. *ECS Transactions* (2009), 25(1, Proton Exchange Membrane Fuel Cells 9), 971-983.
10. P.P. Mukherjee, R. Mukundan, J.S. Spendelow, J.R. Davey, R.L. Borup, D.S. Hussey, D.L. Jacobson, M. Arif, High resolution neutron imaging of water in the polymer electrolyte fuel cell membrane. *ECS Transactions* (2009), 25(1, Proton Exchange Membrane Fuel Cells 9), 505-512.
11. R. Mukundan, R.W. Lujan, J.R. Davey, J.S. Spendelow, D.S. Hussey, D.L. Jacobson, M. Arif, R.L. Borup, Ice formation in PEM fuel cells operated isothermally at sub-freezing temperatures. *ECS Transactions* (2009), 25(1, Proton Exchange Membrane Fuel Cells 9), 345-355.
12. Y. Wang, J. Mishler, P.P. Mukherjee, R. Mukundan, R.L. Borup, Pseudo one-dimensional analysis of polymer electrolyte fuel cell cold-start. *ECS Transactions* (2009), 25(1, Proton Exchange Membrane Fuel Cells 9), 285-294.
13. R. Mukundan, R.L. Borup, Visualising Liquid Water in PEM Fuel Cells Using Neutron Imaging. *Fuel Cells* (Weinheim, Germany) (2009), 9(5), 499-505.
14. A. Nandy, F. Jiang, S. Ge, C.-Y. Wang, and K.S. Chen, **Effect of cathode pore volume on PEM fuel-cell cold start**, *Journal of The Electrochemical Society*, 157 (5) 1-XXXX (2010).
15. F. Jiang, Chao-Yang Wang, and K.S. Chen, **Current ramping: a strategy for rapid start-up of PEMFCs from subfreezing environment**, *Journal of The Electrochemical Society*, 157 (3) B342–B347(2010).
16. M.A. Hickner, K.S. Chen, and S.P. Siegel, **Elucidating Liquid Water Removal in an Operating PEMFC via Neutron Radiography**, *Journal of Fuel Science and Technology*, February 2010, Vol. 7, p.011001-1.
17. S. Basu, C.-Y. Wang, and K.S. Chen, **Phase change in a polymer electrolyte fuel cell**, *Journal of the Electrochemical Society*, 156 (6) B748-B756 (2009).

References

1. N. Holmström, J. Itonen, A. Lundblad, and G. Lindbergh, *FUEL CELLS*, 7. No. 4, 306 (2007).
2. P.M. Wilde, R. Schweiss, M. Steeb, T. Damjanovic, S.G. Foster, and N. Haak, Abstract 042, Lucerne European Fuel Cell Forum conference, July (2009).
3. G.S. Timmins, E.J.H. Bechara, and H.M. Swartz, *The Journal of Experimental Biology*, 203, 2479 (2000).